Asian Journal of Chemistry; Vol. 27, No. 1 (2015), 301-306

ASIAN JOURNAL OF CHEMISTRY

http://dx.doi.org/10.14233/ajchem.2015.17624

Phosphorus and Boron Co-Modified HZSM-5 Catalyst for Methanol to Conversion of Propylene

AINA XU, HONGFANG MA, HAITAO ZHANG, WEIYONG YING* and DINGYE FANG

School of Chemical Engineering, East China University of Science and Technology, Shanghai 200237, P.R. China

*Corresponding author: Tel./Fax: +86 21 64252192 E-mail: wying@ecust.edu.cn

Received: 19 March 2014; *Accepted*: 28 May 2014; *Published online*: 26 December 2014; AJC-16560

PB-HZSM-5 zeolite was prepared by B-ZSM-5 direct synthesis followed by phosphorus impregnation. The structure and properties of PB-HZSM-5 were characterized by XRD, N_2 adsorption, solid state NMR NH_3-TPD, XRF, ICP-AES, TGA and Py-IR. After modification, the weak acidity on the catalyst increased obviously while the strong acidity decreased to a certain level. In comparison with the conventional HZSM-5, the PB-HZSM-5 catalyst expressed a much higher propylene selectivity and longer catalyst life in the conversion of methanol to propylene reaction. The improved catalyst performance could mostly be attributed to the change in the zeolite structure and the acid sites.

Keywords: HZSM-5, Methanol, Boron, Phosphorus, Methanol to propylene.

INTRODUCTION

Light olefins, such as ethylene, propylene and butylenes, have been largely utilized as the raw materials in petrochemical industry. Especially propylene, in recent years, the production rate of propylene still cannot meet the huge and rapidly increasing market demand[1,2]. Methanol-to-olefins (MTO) and methanol-to-propylene (MTP) processes are promising ways to produce propylene using nonpetroleum resources[3-5]. In the traditional methanol-to-olefins process, ethylene is the main product. Compared to methanol-to-olefins, high propylene selectivity is the most attractive feature for methanol-to-propylene process[6]. But to achieve high selectivity of propylene is still a challenging research topic.

Among all the factors in methanol-to-propylene reaction, the catalyst plays a pivotal role in determining the product distributions[7], thus developing high efficient catalysts has been the research focus for many years. ZSM-5 zeolite catalyst is considered to be one of the best catalysts for converting methanol into light olefins and widely reported. Recent studies reveal a much clearer insight into the reaction aspects[8,9]. The key step in effective conversion of methanol to propylene is how to control the reaction at the olefin formation stage, in which the acidity of the catalyst is crucial. Based on the theory, a lot of work has been done to tune the catalyst activity. According to the previous research results, high silica HZSM-5 zeolite is suitable for methanol-to-propylene, whose moderate acidity in high Si/Al samples could improve the formation of propylene[10]. Besides, phosphorus also has been widely used in the catalytic performance improvement[11,12]. After the catalyst is modified with phosphorus, the concentration and strength of acid sites decrease, among which the strong acid sites decrease most. The studies prove that reducing the strong acid sites could enhance both catalytic stability and the propylene selectivity[11]. Moreover, borosilicates with high weak acid density were applied in different reactions by several researchers[13-16]. In methanol-to-propylene reaction, the B-modification could enhance the catalyst stability, since increasing the weak acid sites could avoid various hydrogen-transfer reactions producing aromatics[17].

In brief, both of the weak and strong acidity is very important in methanol-to-propylene reaction. Reducing the strong acidity while increasing the weak acidity to a certain level might be an effective way to improve the methanol-to-propylene catalytic properties. Although both boron and phosphorus are beneficial to improve the efficiency of HZSM-5, the effect of phosphorus on the acidity and surface structure of B-HZSM-5 catalyst has not been studied thoroughly. Further exploring the interaction between phosphorus and boron could help developing high effective catalyst.

In this work, we designed and prepared a PB-HZSM-5 zeolite catalyst by B-ZSM-5 direct synthesis and phosphorus impregnation. The relationship between the catalyst properties and its activity in methanol-to-propylene reaction was discussed.

EXPERIMENTAL

Catalyst preparation: B-ZSM-5 zeolites were synthesized hydrothermally with colloidal mixtures. Certain amount of silica sol, tetrapropylammonium bromide (TPABr) and

deionized water were mixed by stirring to get a translucent gel. $NaAlO_2$, NaOH and H_3BO_3 were dissolved in deionized water and added to the gel to get the mixture. The obtained mixture with the molar composition of SiO_2: (1/260) Al_2O_3: 0.14TPABr: 0.1Na_2O: 30H_2O: 0.01B_2O_3 (Si/Al = 130) was crystallized at 170 °C for 48 h in the autoclave. The precipitated crystals were filtered, rinsed with deionized water, dried and calcined. And then, the zeolite was twice ion exchanged for 4 h at 80 °C with NH_4NO_3 solution, followed by drying and calcination to obtain the protonated sample, labeled as BHZ. The protonated zeolites were incipient impregnated for 24 h in aqueous solution of H_3PO_4. The loading of phosphorus to the modified catalyst was 0.2 wt. %. Then the catalyst was dried, calcined and designated as PBHZ. The unmodified HZSM-5 with the molar ratio of SiO_2: (1/260) Al_2O_3: 0.14TPABr: 0.1Na_2O: 30H_2O was used as benchmark catalyst and marked as HZ.

Catalyst characterization: The structure of the samples was characterized by powder X-ray diffraction (Rigaku D/Max 2550) with CuK_α radiation. XRD patterns were obtained over a 2θ range of 3-50°. Nitrogen adsorption-desorption isotherms were obtained with Micrometrics ASAP 2020. The total surface area was calculated according to the BET isothermal equation and the micropore volume and surface area were evaluated by *t*-plot method. Temperature-programmed desorption (NH_3-TPD) measurements were carried out on Micrometrics AutoChem II 2920. After pretreatment and NH_3 saturation, NH_3 desorbed from the catalyst sample was monitored by TCD while temperature linearly increased to 600 °C. The ^{27}Al, ^{11}B and ^{31}P MAS NMR spectra were obtained after samples hydration on a Bruker DRX 500 spectrometer, using a 4 mm MAS probe, with sample spinning rate of 4 kHz and at resonance frequencies of 130.3, 160.4 and 202.5 MHz, respectively. The spectra were recorded after single pulse excitation with pulse lengths of 4 μs and delay time of 8.1 μs. The elemental compositions of our catalyst samples were measured by ICP-AES using a Varian 710ES spectrometer. X-ray fluorescence (XRF) analysis was conducted with a Shimadzu Corporation XRF-1800 X-ray fluorescence spectrometer. Thermo gravimetric (TGA) data were recorded in flowing air on NETZSCH STA409PC TG/DTA. Pyridine adsorption infrared spectrum measurements (Py-IR) characterization was performed in a Spectrum 100 spectrometer with a resolution of 4 cm^{-1}. The samples were pressed into self-supporting wafers for 15 mg and were pretreated at vacuum condition (400 °C, 1 × 10^{-3} Pa) for 0.5 h. Pyridine vapor was constantly injected to the cell after the samples cooled to room temperature for 0.5 h. The unabsorbed pyridine was eliminated in vacuum and pyridine desorption was accomplished by heating from room temperature to the setting point (150 or 250 °C). The IR spectrum of the catalyst was recorded from 1700 to 1400 cm^{-1}.

Activity measurements: The methanol-to-propylene reaction was conducted in a fixed-bed reactor at 460 °C under atmospheric pressure. Pure methanol was injected into the reaction system from the constant flux pump, with nitrogen as diluents. The weight hourly space velocity (WHSV) for methanol was 0.33 h^{-1}. The analysis of the gas reaction products were performed on-line gas chromatographs: Agilent GC 6890N (FID, Plot Al_2O_3 /KCl). Aqueous and organic phases in liquid products were separated. The aqueous phase and the organic phase were analyzed with Agilent GC 6820 (TCD, Plot Q) and Agilent 7890A (FID, HP-5), respectively. Both methanol and dimethyl ether (DME) was regarded as reactants in the calculation.

RESULTS AND DISCUSSION

Catalyst characterization: Fig. 1 represents the XRD patterns of the catalysts. These patterns display distinct broad diffraction peaks in 8-10 º and 20-25º, 2θ ranges, all of which are consistent with the typical pattern of the MFI crystal structure[18], with no additional phases. This is in agreement with previous literature[12,16]. The results imply that the phosphorus modifier compounds were finely dispersed in monolayer on the surfaces of ZSM-5. The intensities of the peaks of the modified HZSM-5 samples are slightly weaker, indicating a little low crystallization or a little dealuminization due to boron or phosphorus incorporation.

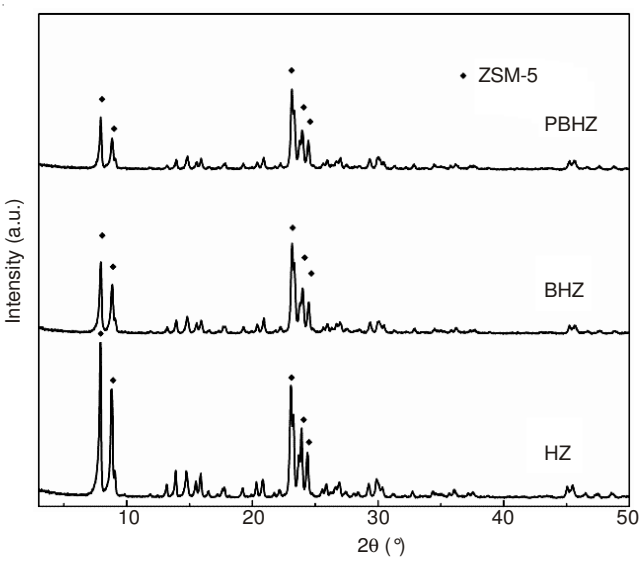

Fig. 1. XRD patterns of the samples

The results of elemental analysis, measured by XRF and ICP-AES, are listed in Table-1. The B/Al ratio of BHZ is much lower than the synthesis gel, which is due to the dissolution of boron species during crystallization[19]. And the boron addition

TABLE-1
TEXTURAL PROPERTIES OF THE SAMPLES

Samples	Si/Al[a]	B/Al[b]	P[b] (wt. %)	S_{BET}[c] (m^2/g)	V_{total}[d] (cm^3/g)	V_{micro}[d] (cm^3/g)
HZ	129	-	-	350	0.21	0.14
BHZ	138	1.35	-	345	0.20	0.13
PBHZ	140	1.46	0.19	341	0.20	0.12

[a]by XRF analysis, [b]by ICP-AES analysis, [c]by the BET method, [d]by the *t*-plot method

reduces the Al amount a little, since the Si/Al ratio of BHZ was higher than HZ. It is proposed that B substitution for Si, during the synthesis, prevents the Al atoms from occupying the T sites. The P content in PBHZ is 0.19 wt. %, which is almost the same as the impregnation amount.

The textural properties, such as surface area and pore volume of the samples, calculated on the basis of nitrogen adsorption, are also listed in Table-1. As shown in Table-1, the addition of boron slightly decreases the surface area, porous volume and microporous volume. After phosphorus impregnation, the surface area and microporous volume of PBHZ are further reduced. It is probably due to the declined crystallinity and the incorporation of boron and phosphorus covers the micropores of zeolite. Actually, all of the structure parameters of the 3 samples are relatively similar, which suggests the textural property is not significantly influenced by boron or phosphorus incorporation.

Information concerning the incorporation and nature of Al in the zeolites has been obtained by ^{27}Al MAS NMR. The ^{27}Al MAS NMR spectra of the zeolites are shown in Fig. 2(a). The intense peak at 55 ppm from tetrahedral coordinate aluminum in the zeolite framework is observed for all samples. With addition of boron in the synthesis mixture and the impregnation of phosphorus on the zeolites successively, the intensity of the peak at 55 ppm decreases consecutively, indicating that the framework aluminum is decreasing. The weak peak at 0 ppm for HZ is due to the extra-framework octahedrally coordinated aluminum[20] and the peak shift to -9 ppm for PBHZ may result from the progressive formation of Al-O-P species on PBHZ[21,22]. The hardly detected extra-framework aluminum indicates that most of the Al of the samples is located in the zeolite frameworks.

Fig. 2(b) shows the ^{11}B MAS NMR spectra of the boron-containing samples. As shown in Fig. 2(b), the main resonance peak assigned to the tetrahedral framework boron at -4 ppm is clearly observed for both samples, while the intensity of the peak for PBHZ is lower than the other. The broad band (8 to -2 ppm) is assigned to the trigonally coordinated B(O-Si)$_3$ in the zeolite framework and the band at 15 ppm is ascribed to the extra-framework trigonally coordinated B[23-26]. These peaks disappear for PBHZ, indicating that phosphorus may slightly remove boron species from both in and out of framework. The peaks on ^{11}B MAS NMR spectra indicate that some certain level of boron atoms have entered the frameworks combining with silicon, which is in good agreement with NH$_3$-TPD results below.

Fig. 2(c) shows the ^{31}P MAS NMR spectra of PBHZ. For PBHZ, several peaks appear at -6, -12, -13, -20, -30 and -36 ppm. The signals at -6 ppm are attributed to phosphorus in pyrophosphoric acid or terminal groups of polyphosphates. The resonances at -12 and -13 ppm can be attributed to species

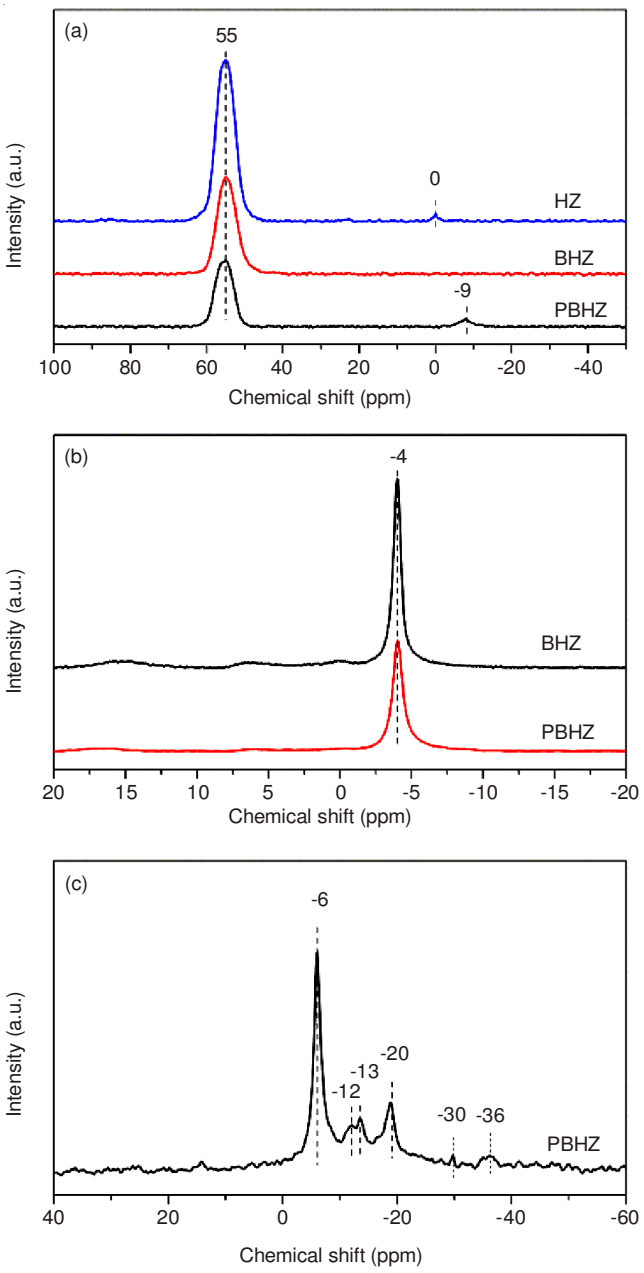

Fig. 2. ^{27}Al MAS NMR (a), ^{11}B MAS NMR (b) and ^{31}P MAS NMR (c) spectra of the catalysts

in the middle groups of polyphosphate chains. The signal at -30 ppm might be assigned to P(BO)$_{4-n}$(SiO)$_n$ structure[27], whose intensity is a little weak because of the small impregnation amount. The resonances at -36 ppm can be attributed to (SiO)$_x$Al(OP)$_{4-x}$[27-30].

The NH$_3$-TPD results of the samples are shown in Fig. 3 and Table-2. The TPD curve exhibits two desorption maxima, which can be assigned to weak and strong acid sites, respec-

TABLE-2
CHEMICAL CHARACTERISATION OF ALL SAMPLES

Samples	Number of acid sites (mmol of NH$_3$/g TPD)					
	T (°C)	Weak	T (°C)	Strong	Total	Coke (wt.%)
HZ	192	0.23	412	0.18	0.41	9.47
BHZ	190	0.50	401	0.14	0.64	2.37
PBHZ	183	0.46	389	0.13	0.59	3.05

tively. For BHZ, the strong acidity decreases while the weak acidity noticeably increases with boron addition, in the mean while, the strong and weak acid strength are both slightly reduced. It clearly emphasizes the effective interaction of boron with the zeolite framework, which means that boron atoms combine with silicon and show weak acidity as BO_3-OH structure[24]. And also boron atoms slightly decreases the formation of strong acid sites by prevent some aluminium atoms from occupying the T sites. Therefore, the acid sites of the boron modified HZSM-5 are different from those of the pure HZSM-5. After phosphorus modification, both the acidity and acid strength of the PBHZ reduce, due to the interaction of phosphorus with zeolite Brønsted acid sites[31,32], including both boron and aluminum Brønsted acid sites.

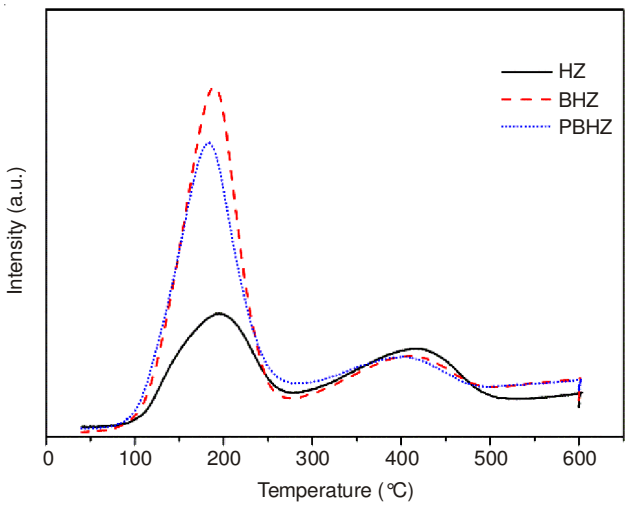

Fig. 3. NH_3-TPD patterns of the samples

The acidity and acid types of the samples are measured by FTIR spectroscopy with pyridine as the probe molecule. The results of the pyridine desorption are summarized in Table-3, at the temperature of 150 and 250 °C. In Table-3, the relative Brønsted and Lewis acidity are determined by the area of the IR bands at 1450 and 1550 cm^{-1}, respectively, using the extinction coefficients by Emeis[33] and assuming the number of Brønsted acid sites of HZ measured at 150 °C to be 100[30]. As shown in Table-3, compared to HZ, the Brønsted acidity of BHZ obviously increases, which indicates the generation of boron Brønsted acid sites after boron addition[13,34,35]. For PBHZ, the phosphorus loading leads to a small reduction in both Brønsted and Lewis acidity. The above results show that the total acidity of the samples, ranked in the sequence of BHZ > PBHZ > HZ, which is in agreement with the results of NH_3-TPD. From Table-3, it also can be seen that in all samples, Brønsted and Lewis acidity decreases with the increasing of

TABLE-3
ACIDITY PROPERTIES OF THE SAMPLES

Samples	Brønsted acidity		Lewis acidity	
	150 (°C)	250 (°C)	150 (°C)	250 (°C)
HZ	100	75	12	8
BHZ	402	350	44	29
PBHZ	382	181	19	11

desorption temperature (from 150 to 250 °C); however, the acidity in the P-modified sample decreases most. The results reveal that P modification has weakened the acid strength of ZSM-5, which also agrees well with the results of NH_3-TPD characterization.

The expected interactions to obtain moderately active sites among modification components in catalyst framework are illustrated in Fig. 4. Firstly, boron atoms enter the frameworks and shown boron Brønsted acid sites after direct synthesis procedure. Subsequently, boron hydroxyl groups react with phosphorus following the impregnation of H_3PO_4, resulting in the formation of B-O-P structure[26]. Furthermore, dehydration interaction also exists between phosphorus and the aluminum hydroxyl groups, with the formation of P-O-Al[31,32].

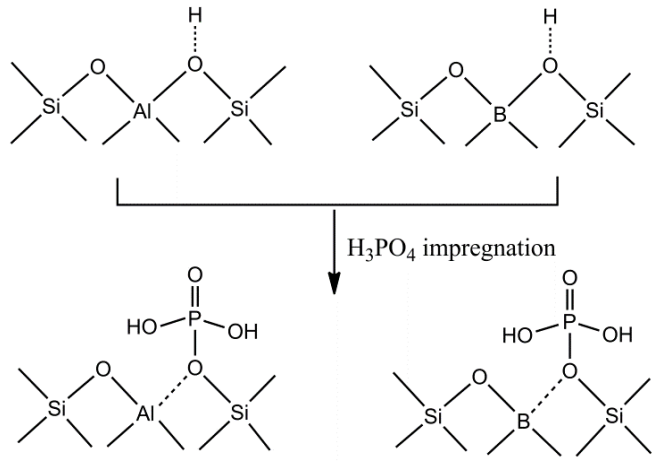

Fig. 4. Scheme of catalyst structure of the modified zeolite

Catalytic activity and stability: The reaction of methanol over unmodified and modified HZSM-5 zeolites was carried out in a fixed-bed reactor. The typical results of the product distributions with different catalysts are displayed in Table-4. The data were recorded after 3 h on stream. The products obtained are classified into light hydrocarbons (C_1-C_4), light olefins ($C_2^=$-$C_4^=$), C_5 and C_6^+ hydrocarbons. The conversions of methanol over all the catalysts were nearly 100 %. On HZ, the high density of strong acid sites, as revealed by the NH_3-TPD study, enhances the hydride transfer and cyclization reactions, resulting in a very high selectivity for C_1-C_4 alkanes.

TABLE-4
CONVERSION OF METHANOL AND HYDROCARBON DISTRIBUTION

Samples	Conversion of methanol (%)	Hydrocarbon Distribution / (mol %)						
		C_{1-4}[a]	C_2H_4	C_3H_6	C_4H_8	C_5	C_6^+[b]	$C_2^=$–$C_4^=$[c]
HZ	99.8	14.48	31.73	26.81	7.11	1.97	17.90	65.65
BHZ	98.7	8.63	32.11	38.03	10.98	1.63	8.62	81.12
PBHZ	99.0	7.37	30.50	44.00	11.35	1.75	5.04	85.85

[a]C_1-C_4 saturated hydrocarbons, [b]C_6 and higher hydrocarbons, [c]$C_2^=$–$C_4^=$ olefins

With boron addition in BHZ, the following changes are observed in the products distribution: Firstly, selectivity of propylene and butylene both increase evidently. Secondly, the C_{1-4} alkanes yields decrease obviously. Thirdly, selectivity of C_6^+ products is decreased apparently. These results suggest that boron in the zeolite framework plays a positive role for improving the selectivity of propylene, which can be attributed to the different catalytic acidity of BHZ, compared to the HZ primary.

After further modification of catalyst by the addition of phosphorus, the propylene selectivity is increased to 44 % while light olefins selectivity to 85.85 % and then the byproducts is further decreased by minimizing the hydride transfer and cyclization reactions, as shown in Table-3. In terms of propylene selectivity this material was considerably better than BHZ.

The catalytic stability of the samples over time on stream (TOS) is shown in Fig. 5(a). HZ displays an initial activity of 98 % but its deactivation is rather fast, as it starts to deactivate within 70 h. The initial activities observed for BHZ and PBHZ are both above 98 % and maintain the stability after more than 120 h. The stability of the boron-incorporated samples is remarkably improved.

Fig. 5(b) shows the propylene selectivity of all samples; it can be seen that the selectivity of propylene over these samples differ visibly. Propylene selectivity of PBHZ and BHZ remain stable within a long period up to about 120 h. As comparison, the selectivity of the sample without B starts to fluctuate apparently and decrease sharply after about 70 h. The propylene selectivity of PBHZ is clearly higher than BHZ. And not only propylene, all the other products selectivity of PBHZ is also stabile (Fig. 5(c)).

From the above results, it is found that the phosphorus impregnated B-HZSM-5 catalyst exhibit high propylene selectivity and long lifetime in the methanol-to-propylene reaction. This performance can be explained from two aspects.

Firstly, the B-HZSM-5 zeolite structure is resistant to coke. It is found that boron contained HZSM-5 catalysts are much more stable than boron-free catalyst. And also, the selectivity of C_6^+ products for HZ was much higher than BHZ and PBHZ, which leads to coking and accelerates the deactivation process as a result. The conclusion can also be verified by TGA results. From TGA results in Table-2, we find that the coking levels for BHZ and PBHZ after 120 h on stream are much lower than that of HZ after 80 h on stream, while the conversions of methanol are almost the same (Fig. 5). This indicates that the generating rate of cokes on the boron contained catalysts is lower. The reason is that the favorable zeolite structure of the catalysts obtained by B directly synthesized, since the weak acid sites were proved to show good anti-coking capability[16].

Secondly, phosphorus impregnation could increase the reaction selectivity. In Table-4, PBHZ greatly improves the propylene selectivity up to 44 % with a high methanol conversion, which is due to the low byproduct selectivity, especially the C_6^+ products amount. After BHZ was modified by P, P species interacts with zeolite Brønsted acid sites[31,32], which further decreases the expression of the catalyst acidity. Considering that the weak acidity on borosilicates is quite high, the influence on strong acidity is more significant. The decrease of strong acidity could successfully suppress the hydride transfer and cyclization reactions which decrease to the formation of aromatics. Thus, with lower content of byproducts, higher selectivity of propylene in methanol-to-propylene reaction is obtained.

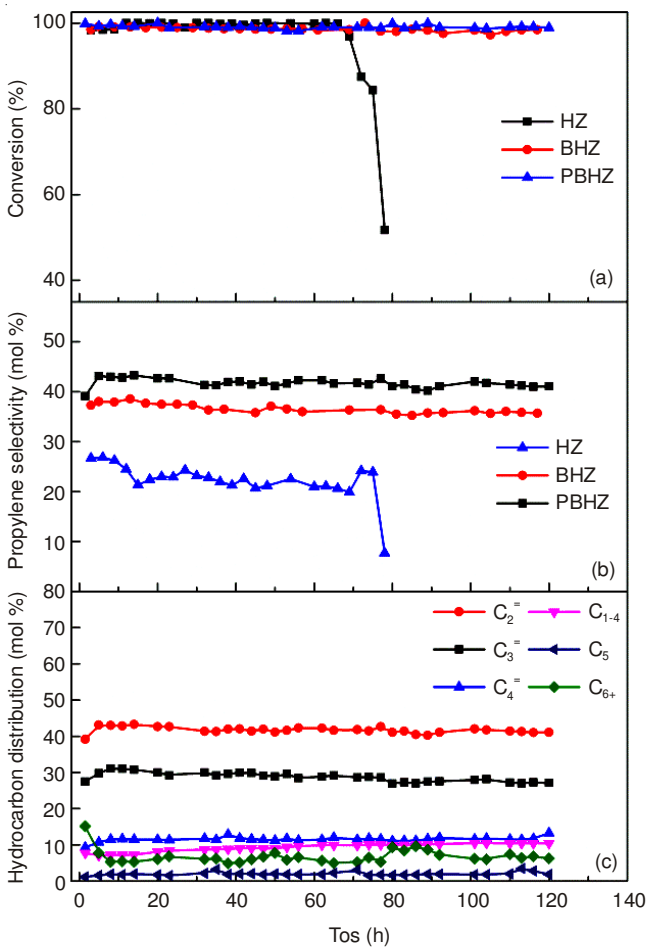

Fig. 5. Conversion of methanol (a), propylene selectivity (b) of the catalysts and product selectivity of PBHZ (c) *versus* time on stream

Conclusion

In this work, boron direct synthesized and phosphorus impregnated PB-HZSM-5 catalyst was well prepared. The characterization results demonstrated that boron atoms in the zeolite framework could increase the catalyst weak acidity and decrease the strong acidity and the interactions between phosphorus atoms and Brønsted acid sites could further decreases the strong acidity. Finally, the modification atoms on the HZSM-5 enhanced the anti-coking capability of the catalyst and reduced the amount of byproducts, which resulted in the enhancement of selectivity for propylene and remarkably prolonged catalytic life in methanol-to-propylene reaction.

ACKNOWLEDGEMENTS

The authors are grateful to the financial support for the National Key Technology Program of China (No. 2006 BAE02 B02).

REFERENCES

1. J.S. Plotkin, *Catal. Today*, **106**, 10 (2005).
2. N. Rane, M. Kersbulck, R.A. Van Santen and E.J.M. Hensen, *Micropor. Mesopor. Mater*., **110**, 279 (2008).
3. M. Stöcker, *Micropor. Mesopor. Mater*., **29**, 3 (1999).
4. J.Q. Chen, A. Bozzano, B. Glover, T. Fuglerud and S. Kvisle, *Catal. Today*, **106**, 103 (2005).
5. M. Hack, U. Koss, P. Konig, M. Rothaemel and H.D. Holtmann, US Patent 7015369 B2 (2006).
6. C. Mei, P. Wen, Z. Liu, H. Liu, Y. Wang, W. Yang, Z. Xie, W. Hua and Z. Gao, *J. Catal*., **258**, 243 (2008).
7. S. Hu, J. Shan, Q. Zhang, Y. Wang, Y.S. Liu, Y.J. Gong, Z. Wu and T. Dou, *Appl. Catal. A*, **445-446**, 215 (2012).
8. S. Svelle, F. Joensen, J. Nerlov, U. Olsbye, K.-P. Lillerud, S. Kolboe and M. Bjørgen, *J. Am. Chem. Soc*., **128**, 14770 (2006).
9. S. Svelle, U. Olsbye, F. Joensen and M. Bjørgen, *J. Phys. Chem. C*, **111**, 17981 (2007).
10. Y.J. Lee, Y.W. Kim, N. Viswanadham, K.W. Jun and J.W. Bae, *Appl. Catal. A*, **374**, 18 (2010).
11. J. Liu, C.X. Zhang, Z.H. Shen, W.M. Hua, Y. Tang, W. Shen, Y.H. Yue and H.L. Xu, *Catal. Commun*., **10**, 1506 (2009).
12. J. Li, Y. Qi, L. Xu, G. Liu, S. Meng, B. Li, M. Li and Z. Liu, *Catal. Commun*., **9**, 2515 (2008).
13. E. Unneberg and S. Kolboe, *Appl. Catal. A*, **124**, 345 (1995).
14. M.B. Sayed and J.C. Védrine, *J. Catal.*, **101**, 43 (1986).
15. Q. Zhu, J.N. Kondo, T. Yokoi, T. Setoyama, M. Yamaguchi, T. Takewaki, K. Domen and T. Tatsumi, *Phys. Chem. Chem. Phys*., **13**, 14598 (2011).
16. Y. Yang, C. Sun, J. Du, Y. Yue, W. Hua, C. Zhang, W. Shen and H. Xu, *Catal. Commun*., **24**, 44 (2012).
17. Q. Zhu, J.N. Kondo, T. Setoyama, M. Yamaguchi, K. Domen and T. Tatsumi, *Chem. Commun.*, **41**, 5164 (2008).
18. Ch. Baerlocher, L.B. McCusker and D.H. Olson, Atlas of Zeolite Framework Types, Academic Press: Elsevier, New York (2007).
19. W. Hölderich, H. Eichhorn, R. Lehnert, L. Marosi, W. Mross, R. Reinke, W. Ruppel and H. Schlimper, in eds.: D.H. Olson and A. Bisio, Proceedings of 6th Intern. Zeol. Conf., Pergamon Press, Butterworths, Guilford, London, p. 545 (1984).
20. P. Sazama, B. Wichterlova, J. Dedecek, Z. Tvaruzkova, Z. Musilova, L. Palumbo, S. Sklenak and O. Gonsiorova, *Micropor. Mesopor. Mater*., **143**, 87 (2011).
21. S.M. Cabral de Menezes, Y.L. Lam, K. Damodaran and M. Pruski, *Micropor. Mesopor. Mater.*, **95**, 286 (2006).
22. G. Zhao, J. Teng, Z. Xie, W. Jin, W. Yang, Q. Chen and Y. Tang, *J. Catal*., **248**, 29 (2007).
23. S.-J. Hwang, C.-Y. Chen and S.I. Zones, *J. Phys. Chem. B*, **108**, 18535 (2004).
24. R. de Ruiter, A.P.M. Kentgens, J. Grootendorst, J.C. Jansen and H. van Bekkum, *Zeolites*, **13**, 128 (1993).
25. W.Y. Dong, Y.J. Sun, H.Y. He and Y.C. Long, *Micropor. Mesopor. Mater*., **32**, 93 (1999).
26. V.R. Reddy Marthala, W. Wang, J. Jiao, Y. Jiang, J. Huang and M. Hunger, *Micropor. Mesopor. Mater*., **99**, 91 (2007).
27. J. Gu, X. Zhang, J. Wang, J. Xu, F. Deng and Z. Yuan, *Stud. Surf. Sci. Catal*., **174**, 209 (2008).
28. K. Damodarana, J.W. Wiench, S.M. Cabral de Menezes, Y.L. Lam, J. Trebosc, J-P. Amoureux and M. Pruski, *Micropor. Mesopor. Mater*., **95**, 296 (2006).
29. K. Ramesh, L.M. Hui, Y.F. Han and A. Borgna, *Catal. Commun*., **10**, 567 (2009).
30. T. Blasco, A. Corma and J. Martineztriguero, *J. Catal*., **237**, 267 (2006).
31. J.C. Vedrine, A. Auroux, P. Dejaifve, V. Ducarme, H. Hoser and S. Zhou, *J. Catal.*, **73**, 147 (1982).
32. W.W. Kaeding and S.A. Butter, *J. Catal*., **61**, 155 (1980).
33. C.A. Emeis, *J. Catal*., **141**, 347 (1993).
34. R. Baran, Y. Millot, T. Onfroy, J.-M. Krafft and S. Dzwigaj, *Micropor. Mesopor. Mater*., **163**, 122 (2012).
35. R. Millini, G. Perego and G. Bellussi, *Top. Catal*., **9**, 13 (1999).